



Microcalorimetry and spectroscopic studies on the binding of dye janus green blue to deoxyribonucleic acid

Baishakhi Saha¹ · Gopinatha Suresh Kumar¹

Received: 8 November 2014 / Accepted: 5 April 2015 / Published online: 30 April 2015
© Akadémiai Kiadó, Budapest, Hungary 2015

Abstract The interaction of the phenazinium dye janus green blue (JGB) with deoxyribonucleic acid was investigated using isothermal titration calorimetry and thermal melting experiments. The calorimetric data were supplemented by spectroscopic studies. Calorimetry results suggested the binding affinity of the dye to DNA to be of the order of 10^5 M^{-1} . The binding was predominantly entropy driven with a small negative favorable enthalpy contribution to the standard molar Gibbs energy change. The binding became weaker as the temperature and salt concentration was raised. The temperature dependence of the standard molar enthalpy changes yielded negative values of standard molar heat capacity change for the complexation revealing substantial hydrophobic contribution in the DNA binding. An enthalpy–entropy compensation behavior was also observed in the system. The salt dependence of the binding yielded the release of 0.69 number of cations on binding of each dye molecule. The non-polyelectrolytic contribution was found to be the predominant force in the binding interaction. Thermal melting studies revealed that the DNA helix was stabilized against denaturation by the dye. The binding was also characterized by absorbance, resonance light scattering and circular dichroism spectral measurements. The binding constants from the spectral results were close to those obtained from the calorimetric data. The energetic aspects of the interaction of the dye JGB to double-stranded DNA are supported by strong binding revealed from the spectral data.

Keywords Janus green blue · DNA · Binding · Interaction · Thermodynamics · Spectroscopy

Introduction

Studies on the interaction of small molecules to nucleic acids continue to evoke considerable interest for rational drug design leading to the development of effective therapeutic molecules particularly anticancer and antiviral agents. In this endeavor understanding the toxicity of such therapeutic molecules to humans is also an important aspect that requires serious attention and sustained investigation. A number of small molecule dyes are useful for intravital coloration of living cells, staining tissues and microorganisms, and consequently, they are in constant interaction with tissues of the human body. Useful application of dyes also involves stimulants of epithelial growth, determination of DNA and RNA content, detection of early invading tumors, fluorescence identification of microorganisms, etc. A number of dyes of phenazinium and phenothiazinium groups have been studied for their strong nucleic acid-binding aspects in realizing their therapeutic potential [1–10].

Janus Green Blue (JGB, Fig. 1) is a dye of the azine azo group (contains both azine and azo chromophores) used as a vital stain in histology. It is useful for staining mitochondria wherein a color change occurs depending upon the amount of oxygen present [11]. It has been utilized in studies for effective and rapid staining of insect chordotonal organs and peripheral nerves [12]. It has also been shown to be an effective agent for the transport of metal ion, particularly Cu(II) through liquid membrane by forming ion pair with bulky counter anion [13]. JGB, compared to many other dyes, has been reported to be unique for its conspicuously higher potency against some clones of *P. Falciparum*, the

✉ Gopinatha Suresh Kumar
gskumar@iicb.res.in; gsk.iicb@gmail.com

¹ Biophysical Chemistry Laboratory, Chemistry Division,
CSIR-Indian Institute of Chemical Biology, 4,
Raja S. C. Mullick Road, Kolkata 700 032, India

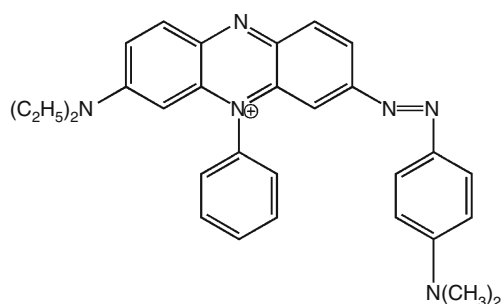


Fig. 1 Chemical structure of the dye janus green blue

malarial parasite [11]. More recently, we reported the binding of this dye to the proteins hemoglobin and myoglobin [14]. Its binding to duplex poly(A) was also studied in our laboratory and was shown to involve intercalation of the dye between the adenine–adenine base pairs [9]. The binding of JGB with nucleic acids, particularly the DNA, has been not yet been investigated in details. Till today there is only one report on its DNA interaction based on the measurement of resonance light scattering [15]. Thus, the molecular aspects of its DNA interaction remain largely obscure although it is very useful in staining nucleic acids [16]. In this investigation, we explored the interaction of JGB with double-stranded DNA using thermochemical techniques, thermal melting, isothermal titration calorimetry and spectroscopic experiments. Characterization of the thermodynamics of small molecule–DNA interactions is very useful in rational drug design protocols [17–20]. Our interest is to provide a detailed interaction profile of this useful dye from calorimetry, thermal melting experiments and spectroscopy.

Experimental

Materials

Calf thymus DNA (CT DNA, highly polymerized, type I, 42 % GC content) from Sigma-Aldrich LLC (St. Louis, MO, USA) was purified by ethanol precipitation. The sample was sonicated to a size of about 200 base pairs and dialyzed into the experimental buffer. The ratio of A_{260}/A_{280} for the DNA sample was around 1.88 indicating the protein free nature of the sample. DNA concentration was determined spectrophotometrically from the absorbance using a molar absorption coefficient (ϵ) value of $13,000 \text{ M}^{-1} \text{ cm}^{-1}$ [21] and expressed per mole of base pairs. JGB (3-diethylamino-7-(4-dimethylaminophenylazo)-5-phenylphenazinium chloride (CAS No. 2869-83-2, Color Index No.11050, Molecular formula: $\text{C}_{30}\text{H}_{31}\text{N}_6\text{Cl}$, purity >86 %) from Sigma-Aldrich was recrystallized twice from alcohol and dried at 40°C in vacuum. The concentration of the dye was determined by an ϵ value of

$38,000 \text{ M}^{-1} \text{ cm}^{-1}$ at 600 nm [22]. No deviation from Beer's law was observed for the dye in the concentration range employed here. The experimental buffer was prepared in MilliQ water from Millipore Water System, Millipore, USA, and filtered through $0.22\text{-}\mu\text{m}$ filters from Millipore, USA, prior to use. All studies were done in 10 mM citrate-phosphate (CP) buffer, pH 6.2 at 20°C as the dye remained positively charged at this pH. For salt-dependent studies, the buffer contained additional $[\text{Na}^+]$ as desired. Temperature-dependent calorimetric studies were performed at 283.15, 293.15 and 303.15 K , respectively. The buffer pH remained unchanged at these temperatures.

Isothermal titration calorimetry

The energetics of the binding of JGB to DNA was measured by using a VP-ITC titration microcalorimeter (MicroCal LLC., Northampton, MA, USA). Prior to the titration experiment, the dye and DNA solutions were degassed extensively on the thermovac unit of the calorimeter. The sample and reference cells of the calorimeter were loaded with the dye solution ($100 \mu\text{M}$) and buffer, respectively. Twenty-eight injections of $10 \mu\text{L}$ each of the DNA solution (1.5 mM) were made into the sample cell containing the dye solution with an interval of 180 s between successive injections. Control experiments of DNA titration into buffer and buffer into dye solution were performed, and the heats generated were subtracted from the dye–DNA injection heats. The corrected isotherms showed that only one type of binding event took place. The isotherms were analyzed using the inbuilt MicroCal ITC software. ‘One set of sites’ model yielded the best-fitted curve for the obtained data points. Equilibrium constant (K) and standard molar enthalpy change (ΔH°) of the association were obtained after fitting each isotherm to the binding model. Standard molar Gibbs energy change (ΔG°) was evaluated using the equation

$$\Delta G^\circ = -RT \ln K \quad (1)$$

$$\Delta G^\circ = \Delta H^\circ - T\Delta S^\circ \quad (2)$$

where R is the universal gas constant ($R = 8.314472 \text{ J K}^{-1} \text{ mol}^{-1}$) and T is the temperature in Kelvin. The standard molar entropy contribution ($T\Delta S^\circ$) was calculated from the standard molar Gibbs energy change of the binding and standard molar enthalpy change according to the above standard thermodynamic relationships.

The first derivative of temperature dependence of enthalpy change was used for the calculation of experimental heat capacity change by using the equation [23]

$$\Delta C_p^{\text{exp}} = \partial \Delta H^\circ / \partial T \quad (3)$$

To determine the extent of enthalpy–entropy compensation, the slope of a plot of ΔH° versus $T\Delta S^\circ$ was

evaluated. The calorimeter was calibrated periodically using water–water and water–methanol dilution experiments as per the protocol provided by MicroCal that the mean energy per injection was $<5.46 \mu\text{J}$ and standard deviation as $<0.063 \mu\text{J}$.

Optical thermal melting studies

Absorbance versus temperature curves (melting profiles) of dye–DNA complexes that depict stabilization of the DNA against thermal strand separation were measured on the Shimadzu unit (Model Pharmaspec 1700) equipped with the peltier-controlled accessory (TMSPC-8, Shimadzu Corporation, Kyoto, Japan) as described earlier [24]. The DNA sample ($40 \mu\text{M}$) was mixed with varying concentrations of the dye in the degassed buffer into the eight chambered 1 cm path length microoptical cuvette. The temperature of the microcell accessory was ramped at a heating rate of 0.5 K min^{-1} , monitoring the absorbance change at 260 nm on the PC. The sigmoidal melting profiles enabled the estimation of melting temperature T_{fus} , the midpoint temperature of the DNA denaturation process.

Spectroscopic studies

Absorption spectral measurements were taken on a Jasco V 660 double-beam double-monochromator spectrophotometer at $20 \text{ }^\circ\text{C}$. Cuvettes of 10 cm path length were used so that aggregation of the dye was prevented. A fixed concentration ($0.65 \mu\text{M}$) of the JGB was titrated against increasing concentration of DNA till saturation in the spectral changes was achieved. The change in absorbance at 624 nm was used to calculate the binding affinity using double reciprocal methodology.

Fluorescence studies

Resonance light scattering (RLS) spectral measurements were taken on a Shimadzu RF 5301-PC spectrofluorimeter unit with right-angle geometry using a 1-cm quartz cell with excitation, and emission bandpass slits set to 5 nm with sensitivity high and response time of 0.25 s. RLS spectra were obtained using the synchronous scanning mode in which the emission and excitation monochromators were preset to identical wavelengths. The excitation and emission monochromator wavelength were adjusted to scan simultaneously through the range from 250 to 600 nm.

Circular dichroism spectroscopy

Circular dichroism (CD) spectra were acquired with a Jasco model J815 spectropolarimeter equipped with a

temperature controller (Jasco International Co., Hachioji, Japan) interfaced with a thermal programmer (425L/15) and controlled by the Jasco software in a rectangular quartz cuvette of 1-cm path length at $20 \pm 0.5 \text{ }^\circ\text{C}$ [25, 26]. Spectra were recorded in the 200- to 350-nm region using a scan speed of 200 nm/min, a bandwidth of 1.0 nm, a response time of 1 s and sensitivity of 100 milli degrees. The DNA ($40 \mu\text{M}$) was titrated with increasing concentration of the dye. Each spectrum was averaged from four successive accumulations and was baseline-corrected and smoothed within permissible limits using the instrument software. The $[\theta]$ values were calculated from the relation, $[\theta] = [\theta]_{\text{obs}}/10lC$. Here $[\theta]_{\text{obs}}$ is the observed ellipticity (milli degrees), C is the molar concentration, and l is the optical path length of the cuvette (cm). The CD spectra are expressed in terms of molar ellipticity $[\theta]$ ($\text{deg. cm}^2 \text{ dmol}^{-1}$) based on base-pair concentration of DNA.

Results and discussion

Isothermal titration calorimetry of dye–DNA interaction

The binding of the dye to the DNA was studied at first from isothermal titration calorimetry. Figure 2 (upper panel) shows the representative raw ITC profiles obtained from dye–DNA titration at 293.15 K. Each heat burst spike in the figure corresponds to the heat generated in a single injection of an aliquot of the DNA into the dye solution. These injection heats were then corrected by subtracting the corresponding dilution heats derived from the injection of identical amount of DNA into the buffer alone (Fig. 2, upper panel, curves offset for clarity). The data revealed that there was only one binding event in the profile and exothermic heats in the process. Therefore, ‘one set of sites’ model yielded the best-fit curve for the obtained data points yielding the thermodynamic parameters of the binding. In Fig. 2 (bottom panel), the resulting corrected heats are plotted against the respective molar ratios. In this panel, the data points are the actual experimental data and the continuous line denotes the calculated fits of the data to the binding model. The binding affinity value and other parameters obtained from ITC are collated in Table 1.

It can be seen that the equilibrium constant of the dye binding to DNA was $(1.97 \pm 0.02) \times 10^5 \text{ M}^{-1}$. The site size (n) value, which is the reciprocal of stoichiometry (N) value, was 2.02. Comparison of the thermodynamic parameters in Table 1 helps to elucidate the forces that govern the complexation. The data showed an overall entropy-driven binding for the dye with a small but favorable enthalpy contribution. The large positive standard molar

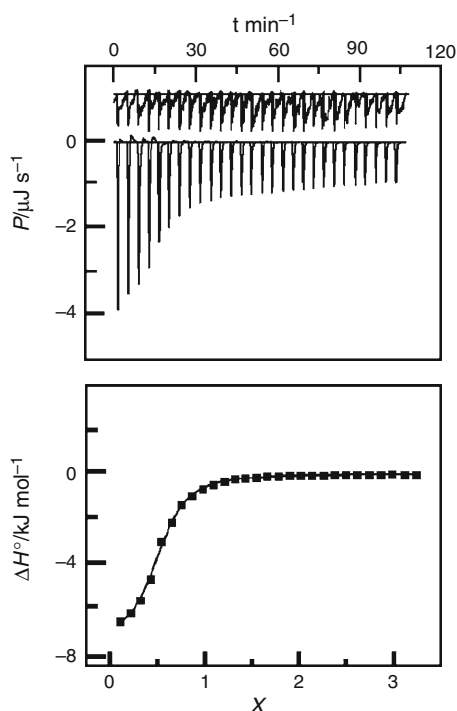


Fig. 2 ITC profile for the titration of DNA (1.5 mM) into a 100 μM solution of JGB (curve at the bottom) along with the dilution profiles (curves on the top offset for clarity). The top panel represents the raw data, and the bottom panel shows the integrated heat data after correction of the heat of dilution. The symbols (square) represent the data points that are fitted to a one set of sites and the solid line is the best-fit data

entropy may essentially originate from the release of bound ions and disrupted water molecules (water of hydration) from the DNA site upon dye binding.

Dependence of ionic strength on the binding reaction

The dye has a positively charge at neutral pH, and therefore, it likely that its binding to the DNA polyanion is thermodynamically linked to the amount of $[\text{Na}^+]$ ions bound to the phosphate groups of the DNA. To understand

the nature of the binding forces involved in the complexation, in particular the role of electrostatic interactions, effect of salt concentration on the binding was investigated by isothermal titration calorimetry experiments in conjunction with van't Hoff analysis. The ITC data in terms of the fitted curves are shown in Fig. 3a. The thermodynamic parameters of the binding at three $[\text{Na}^+]$ concentrations, viz. 10, 20 and 50 mM, were evaluated from ITC experiments, and the results are collated in Table 1. The electrostatic attraction of the cationic dye by the negatively charged phosphate groups of the DNA was reduced with increasing $[\text{Na}^+]$ concentration and the binding affinity diminished. This is clearly evidenced from the decrease in the binding affinity values as seen from the data presented in Table 1; the affinity reduced to less than half on increasing the salt from 10 to 50 mM. The relation between the K values and $[\text{Na}^+]$ has been described previously as

$$\left(\frac{\partial \log K}{\partial \log [\text{Na}^+]} \right)_{T,P} = -z\phi \quad (4)$$

where z is the apparent charge on the bound dye and ϕ is the fraction of sodium ions bound per DNA phosphate group [27–30]. The slope of the linear plot of $\log K$ versus $\log [\text{Na}^+]$ (Fig. 3b) gives the number of cations released on the binding of JGB to the phosphate group of DNA. This value was found to be 0.69 much lower than those reported for mono-cationic ligand molecules binding to DNA and RNA [28]. With increasing salt concentration, the standard molar enthalpy values decreased slightly while the entropy contribution showed little variation.

In order to elucidate the dependence of K on $[\text{Na}^+]$, the observed standard molar Gibbs energy was partitioned between the polyelectrolytic ($\Delta G_{\text{pe}}^{\circ}$) and non-polyelectrolytic ($\Delta G_{\text{t}}^{\circ}$) contributions (Fig. 3c and Table 1). The $z\phi$ value can be used to calculate the polyelectrolytic factor or electrostatic contribution ($\Delta G_{\text{pe}}^{\circ}$) to the overall standard molar Gibbs energy change at a given NaCl concentration by the relation,

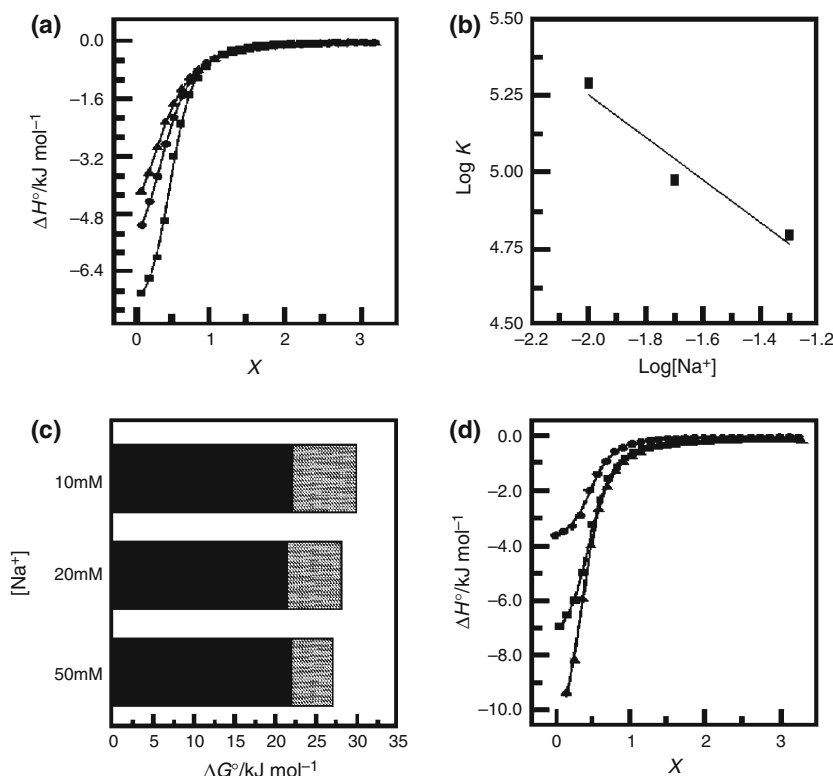
$$\Delta G_{\text{pe}}^{\circ} = -z\phi RT \ln [\text{Na}^+] \quad (5)$$

Table 1 Salt-dependent ITC data for the binding of JGB with DNA

$c[\text{NaCl}]/\text{mM}$	$10^{-5} K/M^{-1}$	$\Delta H^{\circ}/\text{kJ mol}^{-1}$	$T\Delta S^{\circ}/\text{kJ mol}^{-1}$	$\Delta G^{\circ}/\text{kJ mol}^{-1}$	$\Delta G_{\text{pe}}^{\circ}/\text{kJ mol}^{-1}$	$\Delta G_{\text{t}}^{\circ}/\text{kJ mol}^{-1}$
10	1.97 ± 0.02	-7.97 ± 0.06	21.9 ± 0.12	-29.87 ± 0.15	-7.87 ± 0.06	-22.01 ± 0.09
20	0.95 ± 0.01	-6.61 ± 0.05	21.5 ± 0.10	-28.12 ± 0.16	-6.68 ± 0.04	-21.42 ± 0.07
50	0.63 ± 0.01	-6.24 ± 0.05	20.8 ± 0.06	-27.07 ± 0.12	-5.12 ± 0.04	-21.97 ± 0.06

The data in this table are derived from ITC studies at 293.15 K and are average of three determinations. $c[\text{NaCl}]$ is the concentration of NaCl in the solution. K the equilibrium constant and ΔH° the standard molar enthalpy change are determined from ITC profiles fitting to the one set of sites model. The values of $T\Delta S^{\circ}$, the standard molar entropy contribution, and ΔG° , the Gibbs energy change, are determined from relations described in the text. $\Delta G_{\text{pe}}^{\circ}$ and $\Delta G_{\text{t}}^{\circ}$ are the polyelectrolytic and non-polyelectrolytic contributions to ΔG° . Uncertainties correspond to regression of standard errors

Fig. 3 Plot of enthalpy change versus mole ratio showing the integrated heat results of JGB–DNA complexation at **a** 10 (filled square) 20 (filled circle) and 50 (filled triangle) mM $[\text{Na}^+]$ and **d** at $T = 283.15$ K (filled triangle), 293.15 K (filled square) and 303.15 K (filled circle) temperature, respectively. The data are fitted to a ‘one set of sites’ model, and the solid lines represent the best-fit, **b** shows the plot of $\log K$ versus $\log [\text{Na}^+]$ for the binding of JGB with DNA, and **c** represents non-polyelectrolytic (black) (ΔG_i°) and polyelectrolytic (shaded) (ΔG_p°) contribution to ΔG°



where $z\phi$ is the slope of the van't Hoff plot [31, 32]. The difference between the ΔG° and ΔG_{pe}° is the non-polyelectrolytic contribution (ΔG_i°) to the standard molar Gibbs energy change. The ΔG_{pe}° contains enthalpy term originating from coulombic interaction of solute molecules with counter ions present in solution and an entropic term from disordering of the ion atmosphere upon ligand interaction. The ΔG_i° contribution has all other factors such as H-bonding, hydrophobic contacts and van der Waals forces. Thus, ΔG_i° corresponds to the portion of the binding standard molar Gibbs energy change which is independent of salt concentration and contains minimal contribution from polyelectrolyte effects such as coupled ion release. The standard polyelectrolytic contribution to the ΔG° of dye decreased with increase in salt concentration (Table 1). In contrast, the non-polyelectrolytic contribution to the ΔG° was not affected by the salt concentration in the range of Na^+ concentration studied. A graphical representation of the partitioned ΔG° values is shown in Fig. 3c. It is pertinent to note that a significantly lesser contribution of the ionic forces occurred during the binding of JGB to DNA compared to the non-polyelectrolytic forces. This also accounts for the low number of cation expulsion on complexation. Thus, the DNA binding event of JGB is clearly dominated by non-polyelectrolytic process.

Temperature-dependent studies: elucidation of standard molar heat capacity changes

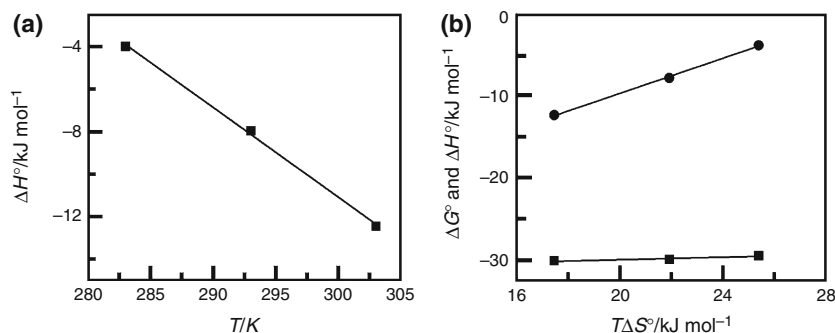
Temperature-dependent ITC experiments were conducted at three different temperatures, viz. 283.15, 293.15 and 303.15 K, respectively. The ITC curves revealed only one binding event at these temperatures. A comparison of the ITC profiles in terms of the fitted curves at the three temperatures is shown in Fig. 3d. As the temperature was increased, the affinity values decreased, the binding enthalpies became more negative with their magnitudes increased. The entropy contribution slightly decreased. The values are presented in Table 2. The variation of ΔH° with T is presented in Fig. 4a, and the value of ΔC_p° obtained from the slope was $0.422 \text{ kJ mol}^{-1}$ (Table 2). A negative ΔC_p° has been suggested to result from the removal of large amount of nonpolar surface from water upon complex formation [33] and is considered as an indicator of the presence of dominant hydrophobic effects in the binding process. Negative values of heat capacity change have been observed for a variety of low molecular weight ligands binding to different nucleic acids [3, 4, 6, 7, 10, 20, 24, 32, 34–36]. The magnitude of ΔC_p° obtained here is close to those frequently observed in many ligand–nucleic acid interactions [34, 35]. Although a number of factors can

Table 2 Temperature-dependent ITC data for the binding of JGB with DNA

T/K	$10^{-5} K/M^{-1}$	$N (1/N)$	$\Delta H^\circ/kJ mol^{-1}$	$T\Delta S^\circ/kJ mol^{-1}$	$\Delta G^\circ/kJ mol^{-1}$	$\Delta C_p/kJ K^{-1} mol^{-1}$
283.15	2.50 ± 0.02	1.85 ± 0.01	-4.01 ± 0.04	25.40 ± 0.15	-29.41 ± 0.15	
293.15	1.97 ± 0.01	2.02 ± 0.01	-7.97 ± 0.05	21.92 ± 0.14	-29.87 ± 0.15	-0.422 ± 0.013
303.15	1.33 ± 0.01	2.99 ± 0.02	-12.45 ± 0.07	17.45 ± 0.12	-30.00 ± 0.16	

The data in this table are derived from ITC studies and are average of three determinations K the equilibrium constant and ΔH° the standard molar enthalpy change are determined from ITC profiles fitting to the one set of sites model. The values of $T\Delta S^\circ$, the standard molar entropy contribution and ΔG° the Gibbs energy change are determined from relations described in the text. Uncertainties correspond to regression of standard errors

Fig. 4 **a** Plot of variation of standard molar enthalpy change (ΔH°) with temperature for the binding of JGB to DNA. **b** Plot of ΔG° (filled square) and ΔH° (filled circle) versus $T\Delta S^\circ$ for the binding of JGB to DNA



contribute to the magnitude of the standard molar heat capacity change of the complexation, change in solvent accessible surface area has been shown to be a significant component [37]. DNA recognition by low molecular weight ligands has been classified as sequence specific, non-specific, minimal sequence specific or structure specific [38]. Small negative ΔC_p° values are considered generally to be the hall mark of systems exhibiting minimal sequence-specific binding [38]. It appears that the negative and nonzero ΔC_p° value observed here for JGB–DNA interaction may be denoting structure-specific binding. The Gibbs energy contribution for the hydrophobic transfer step of binding of JGB to DNA was also calculated from the relationship, $\Delta G_{\text{hyd}}^\circ = (80 \pm 10) \times \Delta C_p^\circ$ [39]. The $\Delta G_{\text{hyd}}^\circ$ value was obtained as $33.76 kJ mol^{-1}$. This value is close to those generally observed for typical DNA and RNA intercalating molecules [6, 34].

Enthalpy–entropy compensation phenomena

The phenomenon of enthalpy–entropy compensation (EEC) is widely invoked as an explanatory principle in thermodynamic analysis of binding of small ligands to macromolecules. Such phenomena may reflect the underlying relation between the standard molar enthalpy and entropy, in particular for relatively flexible interacting systems where a multiplicity of weak interactions occur [40]. It was proposed that EEC is a natural consequence of

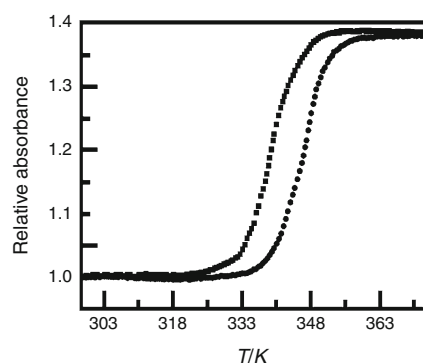


Fig. 5 Optical thermal melting profiles of DNA ($40 \mu M$) (filled square) and JGB–DNA complex at a D/P of 0.5 (filled circle)

the finite heat capacity values. This may occur due to quantum confinement effects, multiple weak interactions and limited free energy windows resulting in thermodynamic homeostasis that may be of evolutionary and functional advantages [41]. It can be seen that as the temperature increased, the ΔH° values increased and the $T\Delta S^\circ$ values decreased, but the ΔG° values remained invariant (Table 2). The reaction enthalpy and entropy, which were strong functions of the temperature, compensated each other to leave the reaction standard molar Gibbs energy more or less independent of temperature. Figure 4b depicts the variations of ΔG° and ΔH° as a function of $T\Delta S^\circ$ for the binding of JGB to DNA. The value of slope

Fig. 6 **a** Absorption spectral changes of JGB (0.65 μM) treated with 0.00, 0.65, 0.20, 0.33, 0.59, 1.11, 2.15, 4.23, 8.39 and 33.48 μM of DNA (curves 1–10). **b** Double reciprocal plot for the JGB–DNA complexation. **c** RLS spectral changes of JGB (10 μM) aggregation in the presence of 0.0, 2.0, 4.0, 6.0, 10.0, 18.0, 34.0 and 66.0 μM of DNA (curves 1–8) of DNA. **d** Scatchard plot of JGB–DNA complexation

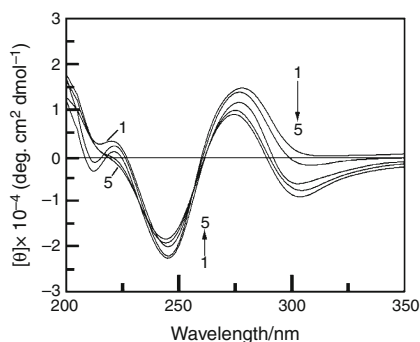
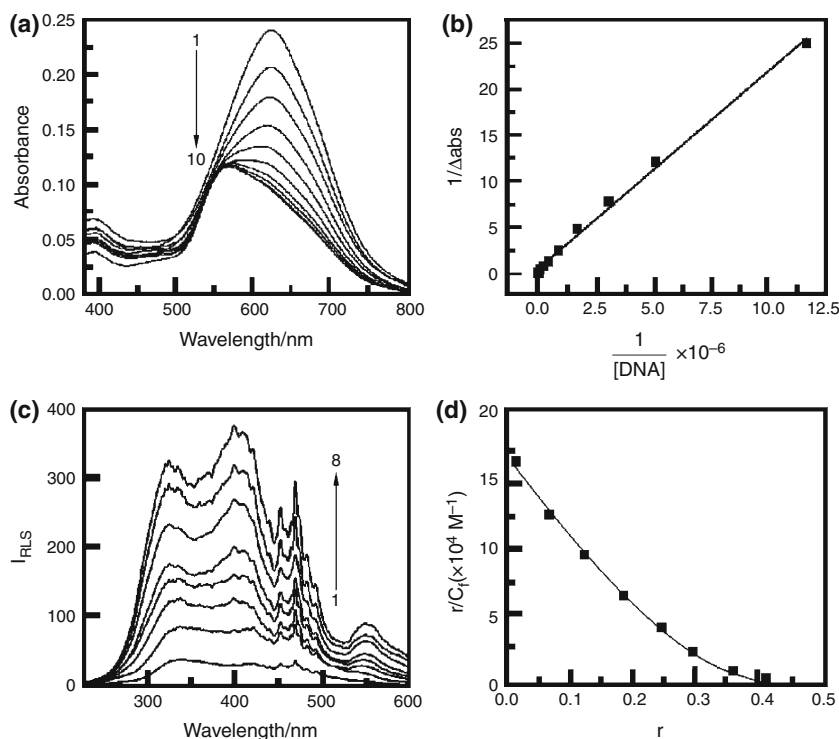


Fig. 7 CD spectral changes of CT DNA (40 μM) (curve 1) treated with 4, 6, 10 and 20 μM of JGB as represented by curves (2–5)

that is $[\partial\Delta H^\circ/\partial(T\Delta S^\circ)]_p$ was 1.05. The linearity of the relationship is an indication of complete EEC. The data obtained here suggest almost complete compensation in all the cases. Enthalpy–entropy compensation is often linked to the solvent reorganization accompanying binding reactions [42]. This ‘temperature-dependent’ enthalpy–entropy compensation is required by basic thermodynamics [43] for any process in which the change in heat capacity ΔC_p° is nonzero. However, the energetics of the interaction indicated significant differences in the molecular forces that contribute and control the binding of JGB to DNA.

DNA optical melting experiments

The ability of the dye to enhance the stability of DNA on binding was investigated from optical melting studies. Stacking interactions of intercalated molecules with the base pairs and the electrostatic interactions resulting from the neutralization of the phosphate charges contribute to the enhancement of the helix melting temperature (T_{fus}). The DNA exhibited an optical melting profile (Fig. 5) with a single transitions at 339.15 K, under the conditions of the present experiment and this is in agreement with the previous reports [44]. The binding of the dye stabilized the DNA structure against denaturation. At saturating concentrations, the T_{fus} of the DNA–dye complex was 345.15 K, an enhancement by about 6 K suggesting strong stabilization of the DNA by the dye. The comparative optical melting profiles are depicted in Fig. 5.

Absorption spectroscopic characteristics of JGB–DNA interaction

We studied the binding of the dye–DNA absorption titration using standard protocols. The characteristic peak for the monomeric JGB at 624 nm (Fig. 6a) underwent a hypochromic effect in the presence of increasing concentration of DNA. This indicates the strong binding of the dye

to the DNA. A similar effect was reported for the binding of the dye to heparin also [45]. These spectral data were quantified using double reciprocal plots (Fig. 6b), and the binding affinity value obtained from the ratio of the intercept to the slope of the plot was $2.10 \times 10^5 \text{ M}^{-1}$. This binding affinity value is close to the binding constant obtained from ITC results. We also determined the stoichiometry of binding by continuous variation method of Job (not shown) and obtained a value of 2.32 in agreement with the 'n' value obtained from ITC data.

Resonance light scattering spectral characteristics on DNA binding

Resonance light scattering is a phenomena of abrupt enhancement of Rayleigh light scattering (RLS) near an absorption band in strongly absorbing chromophores that form large aggregates with strong π -electronic coupling interactions between them [46]. This technique is useful for assignment of dyes and monitors the interaction phenomena. Figure 6c shows the RLS spectra of JGB solution in the range 220–600 nm and in the presence of different concentrations of DNA. It can be seen that the dye at a concentration of 10 μM has a weak RLS signal with a peak at about 560 nm as reported previously [15]. Binding to DNA resulted in an amplified RLS response; the shape and wavelength position of the spectral profile was not effected. The enhancement of the scattering signals occurs due to strong JGB–DNA complex formation. The Scatchard analysis of the RLS data revealed a noncooperative plot (Fig. 6d) with affinity value of $1.70 \times 10^5 \text{ M}^{-1}$. This binding affinity value is close to those obtained from ITC and fluorescence studies.

Conformational changes in JGB–DNA interaction: Circular dichroism spectroscopy results

Circular dichroism spectroscopy is an important tool to understand the changes in the conformation of DNA on interaction with small ligands [2, 25, 26, 42]. We monitored the CD changes in the DNA on interaction of JGB, and the data are shown in Fig. 7. The long-wavelength CD band of the DNA decreased, and concomitant with this change, an induced CD band appeared for the bound dye molecules near 300 nm. These changes reveal the conformational changes in DNA on binding of the dye. However, the 248-nm negative band was less perturbed. Overall, although the conformation of the DNA remained within B-form, the results suggest that the binding of the dye perturbed the DNA conformation apparently due to intercalation.

Conclusions

The thermochemical experiments presented here on the binding of JGB to double-stranded DNA suggested strong exothermic binding. The binding affinity of the dye to 10 mM $[\text{Na}^+]$ was found to be $(1.97 \pm 0.02) \times 10^5 \text{ M}^{-1}$. The reaction was spontaneous ($\Delta G^\circ < 0$), but the affinity became weaker with increasing the salt concentration and temperature. The binding was characterized by a large positive entropy change with a small but favorable enthalpy contribution and revealed an enthalpy–entropy compensation behavior in the temperature range studied. Partition of the Gibbs energy of binding revealed it to consist of a large non-electrostatic contribution although the dye was positively charged at the pH of the study and is known to form ion pair with bulky anions [13]. Negative heat capacity change is correlated with the involvement of significant hydrophobic forces in the complexation. The dye enhanced the thermal stability of DNA as confirmed from melting data, and the binding affinity values deduced from the absorbance data and RLS spectral changes corroborated with those obtained from calorimetry. Conformational changes within B-form were also evidenced from circular dichroism results. Since molecular recognition of DNA by small molecules is an area of significant current interest, the DNA binding results of JGB may be useful to harness its potential for use in biological applications.

Acknowledgements Financial support by the Council of Scientific and Industrial Research (CSIR), Govt. of India, through the network project 'ORIGIN' (CSC0108) is gratefully acknowledged. B. Saha is a NET-Junior Research Fellow of the University Grants Commission, Govt. of India. The authors acknowledge the help and cooperation of the colleagues of the Biophysical Chemistry Laboratory during the course of this work.

References

1. Sarkar D, Das P, Basak S, Chattopadhyay N. Binding interaction of cationic phenazinium dyes with calf thymus DNA: a comparative study. *J Phys Chem B*. 2008;112:9243–9.
2. Das S, Suresh Kumar G. Molecular aspects on the interaction of phenosafranin to deoxyribonucleic acid; model for intercalative drug-DNA binding. *J Mol Struct*. 2008;872:56–83.
3. Saha I, Hossain M, Suresh Kumar G. Sequence-selective binding of phenazinium dyes phenosafranin and safranin O to guanine–cytosine deoxyribopolynucleotides: spectroscopic and thermodynamic studies. *J Phys Chem B*. 2010;114:15278–87.
4. Saha I, Hossain M, Suresh Kumar G. Base pair specificity and energetics of binding of the phenazinium molecules phenosafranin and safranin-O to deoxyribonucleic acids: a comparative study. *Phys Chem Chem Phys*. 2010;12:12771–9.
5. Saha I, Suresh Kumar G. Spectroscopic characterization of the interaction of phenosafranin and safranin o with double stranded, heat denatured and single stranded calf thymus DNA. *J Fluoresc*. 2011;21:247–55.

6. Paul P, Hossain M, Suresh Kumar G. Calorimetric and thermal analysis studies on the binding of phenothiazinium dye thionine with DNA polynucleotides. *J Chem Thermodyn*. 2011;43:1036–43.
7. Saha I, Suresh Kumar G. Phenazinium dyes methylene violet 3RAX and indoline blue bind to DNA by intercalation: evidence from structural and thermodynamic studies. *Dyes Pigments*. 2013;96:81–91.
8. Khan AY, Saha B, Suresh Kumar G. Phenazinium dyes safranin O and phenosafranin induce self-structure in single stranded polyadenylic acid: structural and thermodynamic studies. *J Photochem Photobiol B*. 2014;132:17–26.
9. Khan AY, Saha B, Suresh Kumar G. Interaction of phenazinium dyes with double-stranded poly(A): spectroscopy and isothermal titration calorimetry studies. *Spectrochim Acta A*. 2014;131:615–24.
10. Paul P, Suresh Kumar G. Photophysical and calorimetric investigations on the structural reorganization of poly(A) by phenothiazinium dyes azure A and azure B. *Photochem Photobiol Sci*. 2014;13:1192–202.
11. Vennerstrom JL, Makler TM, Angerhofer CK, Williams J. Antimalarial dyes revisited: xanthenes, azines, oxazines, and thiazines. *Antimicrob Agents Chemother*. 1995;39:2671–7.
12. Field LH, Matheson T. Chordotonal organs of insects. *Adv Insect Physiol*. 1998;27:2–230.
13. Safavi A, Peiravian F, Shams E. A selective uphill transport of copper through bulk liquid membrane using janus green as an anion carrier. *Sep Purif Technol*. 2002;26:221–6.
14. Chatterjee S, Suresh Kumar G. Targeting the heme proteins hemoglobin and myoglobin by janus green blue and study of the dye-protein association by spectroscopy and calorimetry. *RSC Adv*. 2014;4:42706–15.
15. Huang CZ, Li YF, Huang XH, Li M. Interaction of janus green B with double stranded DNA and the determination of DNA based on the measurement of enhanced light scattering. *Analyst*. 2000;125:1267–72.
16. Dutt MK. Basic dyes for the staining of DNA in mammalian tissues and absorption spectra of stained nuclei in the visible light. *Microsc Acta*. 1982;86:59–68.
17. Suresh Kumar G, Debnath D, Sen A, Maiti M. Thermodynamics of the interaction of berberine with DNA. *Biochem Pharmacol*. 1993;46:1665–7.
18. Bhadra K, Maiti M, Suresh Kumar G. Thermodynamics of the binding of cytotoxic protoberberine molecule coralyne to deoxyribonucleic acids. *Biochim Biophys Acta*. 2008;1780:298–306.
19. Das A, Suresh Kumar G. Drug–DNA binding thermodynamics: a comparative study of aristololactam- β -D-glucoside and daunomycin. *J Chem Thermodyn*. 2012;54:421–8.
20. Paul P, Suresh Kumar G. Thermodynamics of the DNA binding of the phenothiazinium dyes toluidine blue O, azure A and azure B. *J Chem Thermodyn*. 2013;64:50–7.
21. Islam MM, Basu A, Hossain M, Suresh Kumar G. Enhanced DNA binding of 9-omega-amino alkyl ether analogs from the plant alkaloid berberine. *DNA Cell Biol*. 2011;30:123–33.
22. Johansson HE, Johansson MK, Wong AC, Armstrong ES, Peterson EJ, Grant RE, Roy MA, Reddington MV, Cook RM. BTII, an Azoreductase with pH-dependent substrate specificity. *Appl Environ Microbiol*. 2011;77:4223–5.
23. Ladbury JE, Williams MA. The extended interface: measuring non-local effects in biomolecular interactions. *Curr Opin Struct Biol*. 2004;14:562–9.
24. Hossain M, Suresh Kumar G. DNA intercalation of methylene blue and quinacrine: new insights into base and sequence specificity from structural and thermodynamic studies with polynucleotides. *Mol BioSyst*. 2009;5:1311–22.
25. Debnath D, Kumar GS, Maiti M. Circular dichroism studies of the structure of DNA complex with berberine. *J Biomol Struct Dyn*. 1993;9:61–79.
26. Kumar GS, Maiti M. DNA polymorphism under the influence of low pH and low temperature. *J Biomol Struct Dyn*. 1994;12:183–201.
27. Record MT Jr, Lohman ML, De Haseth P. Ion effects on ligand nucleic acid interactions. *J Mol Biol*. 1976;107:145–58.
28. Record MT Jr, Anderson CF, Lohman TM. Thermodynamic analysis of ion effects on the binding and conformational equilibria of proteins and nucleic acids: the roles of ion association or release, screening, and ion effects on water activity. *Q Rev Biophys*. 1978;11:103–78.
29. Chaires JB. Energetics of drug-DNA interactions. *Biopolymers*. 1998;44:201–15.
30. Chaires JB. Thermodynamics of the daunomycin-DNA interaction: ionic strength dependence of the enthalpy and entropy. *Biopolymers*. 1985;24:403–19.
31. Record MT Jr, Ha JH, Fisher MA. [16] Analysis of equilibrium and kinetic measurements to determine thermodynamic origins of stability and specificity and mechanism of formation of site-specific complexes between proteins and helical DNA. *Methods Enzymol*. 1991;208:291–343.
32. Chaires JB, Satyanarayana S, Suh D, Fokt I, Przewlaka T, Priebe W. Parsing the free energy of anthracycline antibiotic binding to DNA. *Biochemistry*. 1996;35:2047–53.
33. Spolar RS, Record MT Jr. Coupling of local folding to site-specific binding of proteins to DNA. *Science*. 1994;263:777–84.
34. Islam MM, Roy Chowdhury S, Suresh Kumar G. Spectroscopic and calorimetric studies on the binding of alkaloids berberine, palmatine and coralyne to double stranded RNA polynucleotides. *J Phys Chem B*. 2009;113:1210–24.
35. Roy Chowdhury S, Islam MM, Suresh Kumar G. Binding of the anticancer alkaloid sanguinarine to double stranded RNAs: Insights into the structural and energetics aspects. *Mol BioSyst*. 2010;6:1265–76.
36. Bhowmik D, Buzzetti F, Fiorillo G, Orzi F, Syeda TM, Lombardi P, Suresh Kumar G. Calorimetry and thermal analysis studies on the binding of 13-phenylalkyl and 13-diphenylalkyl berberine analogs to tRNA^{Phe}. *J Therm Anal Calorim*. 2014;118:461–73.
37. Ren J, Jenkins TC, Chaires JB. Energetics of DNA intercalation reactions. *Biochemistry*. 2000;39:8439–47.
38. Murphy FV, Churchill ME. Nonsequence-specific DNA recognition: a structural perspective. *Structure*. 2000;8:R83–9.
39. Ha J, Spolar RS, Record MT Jr. Role of hydrophobic effect in stability of site-specific protein-DNA complexes. *J Mol Biol*. 1989;209:801–16.
40. Guthrie KM, Parenty AD, Smith LV, Cronin L, Cooper A. Microcalorimetry of interaction of dihydro-imidazo-phenanthridinium (DIP)-based compounds with duplex DNA. *Biophys Chem*. 2007;126:117–23.
41. Cooper A, Johnson CM, Lakey JH, Nollmann M. Heat does not come in different colours: entropy–enthalpy compensation, free energy windows, quantum confinement, pressure perturbation calorimetry, solvation and the multiple causes of heat capacity effects in biomolecular interactions. *Biophys Chem*. 2001;93:215–30.
42. Chaires JB. A thermodynamic signature for drug-DNA binding mode. *Arch Biochem Biophys*. 2006;453:26–31.
43. Lee B. Enthalpy-entropy compensation in the thermodynamics of hydrophobicity. *Biophys Chem*. 1994;51:271–7.
44. Bhadra K, Das S, Suresh Kumar G. Protonated structures of naturally occurring deoxyribonucleic acids and their interaction with berberine. *Bioorg Med Chem*. 2005;13:4851–63.
45. Long YJ, Li YF, Huang CZ. A wide dynamic range detection of biopolymer medicines with resonance light scattering and absorption radiometry. *Anal Chim Acta*. 2005;552:175–81.
46. Pasternack RF, Collings PJ. Resonance light scattering: a new technique for studying chromophore aggregation. *Science*. 1995;269:935–9.